Published OnlineFirst June 29, 2010; DOI: 10.1158/1541-7786.MCR-10-0161

Molecular Cancer Research

Functional Characterization of a Cancer Causing Mutation in Human Replication Protein A

Cathy S. Hass[1], Lokesh Gakhar[2], and Marc S. Wold[1]

Abstract

Replication protein A (RPA) is the primary ssDNA-binding protein in eukaryotes. RPA is essential for DNA replication, repair, and recombination. Mutation of a conserved leucine residue to proline in the high-affinity DNA binding site of RPA (residue L221 in human RPA) has been shown to have defects in DNA repair and a high rate of chromosomal rearrangements in yeast. The homologous mutation in mice was found to be lethal when homozygous and to cause high rates of cancer when heterozygous. To understand the molecular defect causing these phenotypes, we created the homologous mutation in the human RPA1 gene (L221P) and analyzed its properties in cells and *in vitro*. RPA1(L221P) does not support cell cycle progression when it is the only form of RPA1 in HeLa cells. This phenotype is caused by defects in DNA replication and repair. No phenotype is observed when cells contain both wild-type and L221P forms of RPA1, indicating that L221P is not dominant. Recombinant L221P polypeptide forms a stable complex with the other subunits of RPA, indicating that the mutation does not destabilize the protein; however, the resulting complex has dramatically reduced ssDNA binding activity and cannot support SV40 DNA replication *in vitro*. These findings indicate that in mammals, the L221P mutation causes a defect in ssDNA binding and a nonfunctional protein complex. This suggests that haploinsufficiency of RPA causes an increase in the levels of DNA damage and in the incidence of cancer. *Mol Cancer Res; 8(7); 1017–26. ©2010 AACR.*

Introduction

Efficient maintenance of the genome is required for cell survival and proliferation. The cell must faithfully replicate billions of bp as well as identify and repair a variety of DNA lesions. Replication protein A (RPA), the major eukaryotic ssDNA binding protein, is required for cell viability and plays essential roles in DNA replication, repair, and recombination (1-3). RPA also plays a role in coordinating DNA metabolism with the cell cycle (4-6). RPA expression is upregulated in tumors including breast and colon cancer and has been shown to play an important role in cell proliferation during cancer growth and progression (7, 8).

The RPA complex binds to ssDNA with high affinity and low sequence specificity (9-11), and interacts with proteins involved in DNA replication, repair, recombination, and checkpoint pathways (3, 6, 12, 13). RPA is a stable three-subunit complex composed of RPA1, RPA2, and RPA3 (1-3). The genes for all three subunits are essential for cell viability and chromosome stability (14, 15); however, the largest subunit, RPA1, is responsible for high affinity ssDNA binding and many protein-protein interactions (3). RPA1 is composed of four structurally related DNA binding domains (DBD; ref. 3). The NH_2-terminal domain DBD-F contains many protein interaction sites involved in DNA repair, recombination, and cell cycle regulation (16). The COOH-terminal domain DBD-C is involved in complex formation with the other RPA subunits and also plays a role in recognizing DNA damage (17, 18). The central two domains DBD-A and DBD-B have the highest DNA affinity in the RPA1 subunit and constitute the ssDNA-binding core of the complex (3, 19-21).

Extensive genetic analysis of the yeast homologue of RPA1 (RFA1) has shown that viable mutations in this gene exhibit defects in DNA repair, recombination, and elevated chromosome rearrangements and mutation rates (15, 22). In mammalian cells, RPA is essential for life, and depletion leads to an accumulation of cells in S phase due to deficient DNA replication and activation of DNA checkpoints due to the persistence of DNA damage (5, 23).

One mutation in RPA1 that has been studied in both yeast and mammals is a leucine to proline substitution at position 221 in DBD-A of the human RPA1 subunit. The mutation is found within a hydrophobic patch at the base of an extended β-ribbon region in DBD-A near the RPA-DNA interface. The L221P mutation was first described in a yeast mutagenesis screen and exhibited sensitivity to DNA-damaging agents, defects in checkpoints

Authors' Affiliations: [1]Department of Biochemistry and [2]Protein Crystallography Facility, Carver College of Medicine, University of Iowa

Corresponding Author: Marc S. Wold, 375 Newton Road, 3107 MERF, Iowa City, IA 52242. Phone: 319-335-6784; Fax: 319-384-4770. E-mail: marc-wold@uiowa.edu

doi: 10.1158/1541-7786.MCR-10-0161

Published OnlineFirst June 29, 2010; DOI: 10.1158/1541-7786.MCR-10-0161

and homologous recombination, and gross chromosomal rearrangements (22, 24). However, no evidence for a major defect in DNA replication was observed. Homozygous expression of the L221P mutant RPA1 in mice was shown to be embryonic lethal. The heterozygous mice were viable but had shortened life spans and elevated cancer rates (25). The tumors were found to have widespread chromosomal rearrangements similar to those found in human cancers (25).

To understand the molecular defect causing chromosomal instability, the equivalent L221P mutation was made and characterized in human RPA1. A knockdown/reconstitution system in HeLa cells was used to assess its function in human cells. Cells containing only RPA1 (L221P) exhibit abnormal cell cycle progression characterized by an accumulation in S and G_2-M phases. Studies with synchronized cellular populations showed that RPA1(L221P) is unable to support S-phase progression indicating a replication defect. The mutant protein was unable to localize to damage-induced sites of DNA repair in cells, suggesting it is also defective in DNA repair. Studies in cells expressing both wild-type (WT) and mutant forms of RPA1 indicated that the L221P form is not dominant. Biochemical analysis with recombinant RPA1(L221P) showed that the mutant subunit is able to associate with the other two subunits in a stable complex but is unable to bind ssDNA or support *in vitro* replication. These results indicate that the L221P mutation disrupts RPA ssDNA-binding function resulting in a nonfunctional complex. These studies indicate that haploinsufficiency of RPA caused by the expression of a defective form of RPA results in genomic instability.

Materials and Methods

Construction of RPA1(L221P)

For the cell culture studies, a previously constructed enhanced green fluorescent protein (GFP)–tagged version of RPA1 (23) was modified using quick-change site-directed mutagenesis to mutate leucine 221 to proline. Primers used were 5′-CCAGTTCTAGGGAGAAAGGCTTC-CCTTCCCC-3′ and 5′-GGGGAAGGGAAGCCTTT-CTCCCTAGAACTGG-3′.

RNAi knockdown and replacement of RPA1

Method for knockdown of endogenous RPA1 and expression of exogenous RPA1 was as described (23). HeLa cells (obtained from the American Type Culture Collection) grown in DMEM with 10% calf serum at 37°C with 5% CO_2 were seeded in six-well tissue culture plates at 2×10^5 cells per well. Small interfering RNA (siRNA) (200 pmol) was added 24 hours after seeding the plates to knockdown endogenous RPA1. Transfections were done with 5 μL of Lipofectamine 2000 (Invitrogen). At 24 hours after transfection of siRNA, cells were transfected with 250 ng of plasmids expressing GFP fusions of WT or mutant RPA1. The RPA1 siRNA target sequence was 5′-GGAAU-UAUGUCGUAAGUCA-3′.

Flow cytometry analysis

Cells were collected at 96 hours posttransfection of siRNA, washed with PBS, and fixed overnight in 70% methanol. The cells were rehydrated in PBS for 30 minutes and washed in PBS. For cell cycle analysis, 0.1 mg/mL propidium iodide was added to each sample. For analysis of ChK2 activation, cells were incubated in 1:100 p-ChK2 primary antibody (Cell Signaling) overnight then in 1:100 phycoerythrin secondary (Invitrogen) for 2 hours. Cells were examined on a FACScan II, and the data were analyzed using the FlowJo software (TreeStar).

Immunofluoresence analysis

HeLa cells were seeded on coverslips in six-well tissue culture plates, and subjected to RNAi knockdown and replacement of RPA1 as described above (23, 26). At 92 hours posttransfection of siRNA, 20 μmol/L camptothecin was added to each well. The cells were incubated for 4 hours at 37°C and 5% CO_2. Coverslips were washed twice in cold CSK buffer (10 mmol/L HEPES, 300 mmol/L sucrose, 100 mmol/L NaCl, and 3 mmol/L $MgCl_2$). Nonchromatin-bound RPA was extracted with CSK/0.5% Triton X-100 for 5 minutes. Coverslips were fixed with 4% formaldehyde for 20 minutes then washed thrice with PBS. To detect RPA2 or phosphorylated H2AX (p-H2AX), coverslips were incubated in blocking solution (5% calf serum, PBS) for 1 hour at room temperature then primary antibody for RPA2 (71-9A) or p-H2AX (Cell Signaling) at 1:500 overnight at 4°C. Coverslips were washed thrice with PBS then incubated in anti-rabbit Texas red secondary antibody (Cell Signaling) at 1:800 for 2 hours. Coverslips were washed in PBS, incubated in DNA staining solution (1 μg/μL 4′,6-diamidino-2-phenylindole), washed again in PBS, and mounted to slides. Slides were examined with a Leica immunofluorescence microscope, and images were collected with SPOT software (Diagnostic Instruments, Inc.). Adobe Photoshop was used to process and overlay images.

Purification of recombinant RPA complex

WT and L221P mutant RPA complexes were expressed in BL21(DE3) and purified as described in Binz et al. (26).

SV40 replication and ssDNA binding reactions

Reactions were carried out as previously described (26). Briefly, 25 μL SV40 reactions contained 30 mmol/L HEPES (pH 7.5); 7 mmol/L $MgCl_2$; 40 mmol/L creatine phosphate; 2.5 μg creatine kinase; 4 mmol/L ATP; 0.2 mmol/L each of CTP, GTP, and UTP; 0.1 mmol/L each of dATP, dGTP, and dTTP; 0.05 mmol/L α32-P-dCTP; 50 ng pUC•HSO DNA template; and 6 μL RPA-depleted HeLa cytosolic extract. HeLa cell extract was depleted of RPA using 35% to 65% ammonium sulfate fractionation (27). SV40 T-antigen (1.9 μg; Chimex) and 400 ng of purified WT or L221P mutant RPA were added as indicated. Reactions were incubated for 2 hours at 37°C. Reactions were quenched by addition of 0.1 mol/L sodium pyrophosphate, precipitated with 10% trichloracetic acid, and

Published OnlineFirst June 29, 2010; DOI: 10.1158/1541-7786.MCR-10-0161

DNA filtered through glass microfiber filters. The amount of synthesized radiolabled DNA was quantified by scintillation counting.

ssDNA binding reactions contained 30 mmol/L HEPES, 100 mmol/L NaCl, 5 mmol/L $MgCl_2$, 0.5% inositol, 1 mmol/L DTT, 2 fmol labeled $(dT)_{30}$, bovine serum albumin (50 ng/μL), and 0 to 316 fmol of mutant or WT RPA. Reactions were incubated for 20 minutes at 25°C and then separated on a 1% agarose gel in 0.1× TAE buffer (4 mmol/L Tris acetate and 0.2 mmol/L EDTA). Position of free and bound DNA was quantified using a Packard Instant Imager, and the fraction of free ssDNA was plotted against RPA concentration. The data were analyzed by nonlinear least squares fitting to the Langmuir binding equation using KaleidaGraph (Synergy) to calculate the apparent binding constant (11).

Results

L221 is highly conserved in evolution

The leucine at position 221 in DBD-A of human RPA1 is highly conserved. This residue is absolutely conserved in animals and some unicellular eukaryotes including yeast (Table 1). In RPA1 homologues in which the leucine is not present (some plants and unicellular eukaryotes), the leucine is replaced with another hydrophobic residue. This conservation suggests that this residue is important for some aspect of RPA1 structure or function. L221 is located near the base of the β2 strand of the β sheet that forms the DNA-binding surface of DBD-A (Fig. 1A; refs. 20, 28). Although L221 does not seem to interact directly with DNA, the leucine side chain does extend toward the DNA in the crystal structure (Fig. 1A; ref. 28), and nuclear magnetic resonance analysis indicated that the chemical environment of L221 changes upon DNA binding (20). Conversion of leucine to a conformationally constrained proline residue is predicted to disrupt the β sheet, which is the core of the DNA binding site in DBD-A (Fig. 1B).

RPA1(L221P) is unable to rescue cell cycle progression

We initially wished to directly determine whether RPA1 containing the leucine to proline mutation at position 221 could function in human cells. We have previously established protocols for using siRNA knockdown/exogenous gene reconstitution to examine RPA1 function in cells (23). HeLa cells are treated with a siRNA targeted to the 3′ untranslated region of RPA1 that causes endogenous RPA1 levels to decrease to <5% of normal levels (23). Twenty-four hours after transfection of siRNA, plasmid expressing different forms of RPA1 lacking the targeted 3′ untranslated region fused to GFP were introduced into the cells, and the distribution of cells in the cell cycle was determined by flow cytometry analysis after propidium iodide staining of DNA.

Table 1. Alignment of L221 residue of RPA1 subunit from various species

Species, accession number	Start	Sequence	Stop
Homo sapiens NP_002936.1	183	KVVPIASLTPYQSKWTICARVTNKSQIRTWSNSR-GEGK**L**FSLELVD-ESG	231
Pan troglodytes XP_511254.2	237	KVVPIASLTPYQSKWTICARVTNKSQIRTWSNSR-GEGK**L**FSLELVD-ESG	285
Canis lupus familiaris XP_868487.1	181	KVVPIASLTPYQSKWTICARVTNKSQIRTWSNSR-GEGK**L**FSIELVD-ESG	229
Bos taurus NP_001068644.1	183	KVVPIASLTPYQSKWTICARVTNKSQIRTWSNSR-GEGK**L**FSIELVD-ESG	231
Mus musculus NP_080929.1	192	KVVPIASLTPYQSKWTICARVTNKSQIRTWSNSR-GEGK**L**FSLELVD-ESG	240
Rattus norvegicus XP_213389.4	183	KVVPIASLTPYQSKWTICARVTNKSQIRTWSNSR-GEGK**L**FSIELVD-ESG	231
Gallus gallus NP_001006221.1	180	KVVPIASLNPYQSKWTICARVTQKGQIRTWSNSR-GEGK**L**FSIELVD-ESG	228
Danio rerio NP_956105.2	170	KVVPIASLNPYQSKWTIRARVTNKSAIRTWSNSR-GDGK**L**FSMELVD-ESG	218
Drosophila melanogaster NP_524274.1	168	---PISSLSPYQNKWVIKARVTSKSGIRTWSNAR-GEGK**L**FSMDLMD-ESG	213
Anopheles gambiae XP_321709.3	179	---PISSLSPYQNKWVIKARVMSKSGIRTWSNAK-GEGK**L**FSMDVMD-ESG	224
Schizosaccharomyces pombe NP_595092.1	178	IIYPIEGLSPYQNKWTIRARVTNKSEVKHWHNQR-GEGK**L**FSVNLLD-ESG	226
Saccharomyces cerevisiae NP_009404.1	183	PIFAIEQLSPYQNVWTIKARVSYKGEIKTWHNQR-GDGK**L**FNVNFLD-TSG	231
Kluyveromyces lactis XP_451388.1	187	PIFAIEQISPYQNNWTIKARVSFKGDLKKWQNNR-GEGH**I**LNVNLLD-SSG	235
Eremothecium gossypii NP_985540.1	261	PIFAIEQLSPYQNMWTIKARVSFKGDIKTWHNQR-GEGK**L**FNVNFLD-TSG	309
Magnaporthe grisea XP_368559.1	178	NIYPIESISPYQHKWTIKARVSQKSDIRTWHKAS-GEGK**L**FSVNLLD-ETG	226
Neurospora crassa XP_322908.1	173	TIYPIEGLSPFSHKWTIKARVTSKSDIKTWHKAS-GEGK**L**FSVNFLD-ESG	221
Arabidopsis thaliana NP_567576.2	227	KIIPVNALSPYSGRWTIKARVTNKAALKQYSNPR-GEGK**V**FNFDLLDADGG	276
Arabidopsis thaliana NP_199353.1	298	RINPIAALNPYQGRWTIKVRVTSKADLRRFNNPR-GEGK**L**FSFDLLDADGG	347
Oryza sativa NP_001054445.1	306	RIIPITALNPYQPKWTIKARVTAKSDIRHWSNAR-SSGT**V**FSFDLLDAQGG	355
Cryptosporidium parvum(short) AAD42062.1	1	MPIREVNVNRQTISIKGRIIQKSSLQIL---K-SGLR**F**FHLDIIDKDND	45
Cryptosporidium parvum(long) AAW71479.1	191	PVYPIKNITSYLHRWRIVGRVVSKSDIRKFSSSKTKEGK**V**FSFEICDADGS	240

NOTE: Selected residues of DBD-A in RPA1 from various organisms are shown. L221 and the homologous residues are in bold.

Published OnlineFirst June 29, 2010; DOI: 10.1158/1541-7786.MCR-10-0161

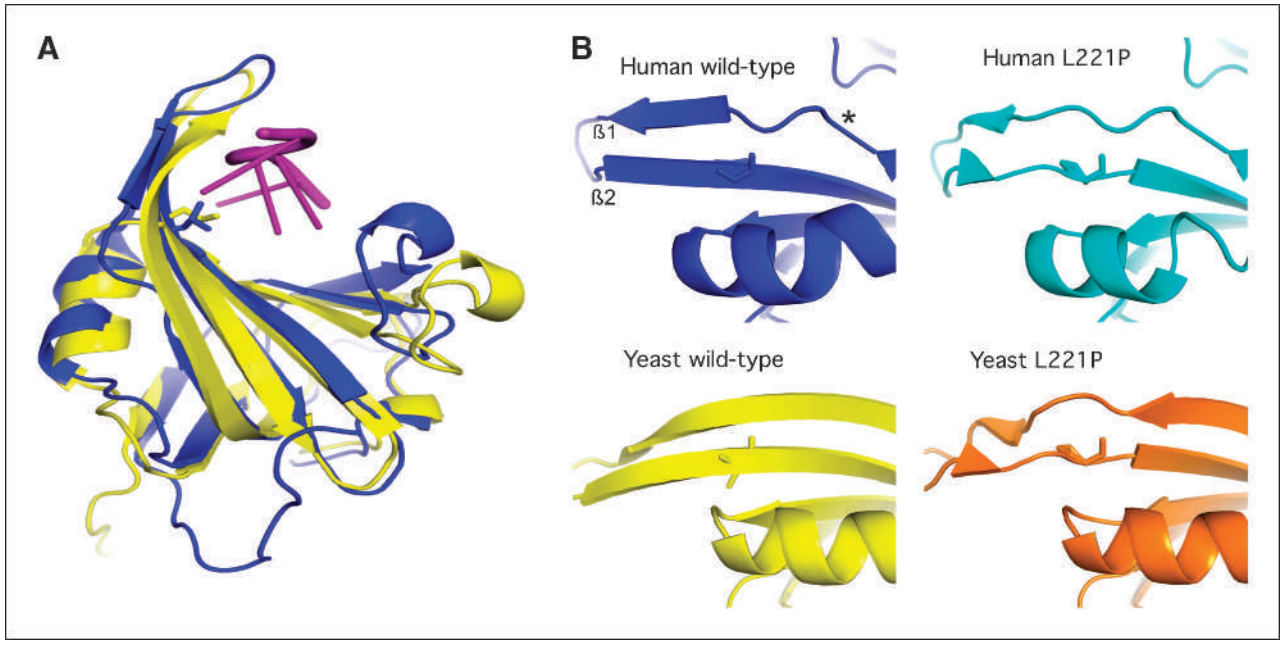

FIGURE 1. Structures and modeling of WT and L221P. A, structures of DBD-A from WT human RPA1 (blue) bound to DNA (magenta; 1JMC; ref. 28) and yeast RPA1 (yellow; 1YNX; ref. 39). Position of L221 side chain is shown extending toward DNA from left side of binding cleft. B, β1 and β2 strands of the DNA binding site shown for (left) structures of WT human and yeast, and (right) modeled structures of human and yeast L221P. Shown from outside looking toward the DNA centered on position 221. β1 and β2 are labeled and the discontinuity in the human structure is indicated (*). Models were determined using Modeller (from structures shown in A; ref. 40). DSSP was used for secondary structure assignment (41); structures were rendered in PyMOL.

Optimal knockdown of endogenous RPA1 and expression of exogenous RPA1 occurred between 96 and 120 hours after siRNA transfection (data not shown; ref. 23). As has been observed previously, knockdown of endogenous RPA1 causes an accumulation of cells in the S and G_2-M phase (Fig. 2A, compare left two panels; refs. 5, 23). This phenotype is caused by defects in DNA replication and repair. Expression of the exogenous form of RPA1 was monitored by green fluorescence, and only GFP-expressing cells were selected for analysis in the reconstitution experiments. GFP-tagged WT RPA1 was able to rescue RPA1-depleted cells to give a normal cell cycle distribution with the majority of cells in the G_1 phase and a moderate G_2-M peak (Fig. 2A, third panel). The GFP-RPA1 expression plasmid was mutated at position 221 to produce a leucine to proline substitution. The resulting GFP-RPA1(L221P) was also expressed in RPA1-depleted cells. In contrast to WT RPA1, expression of GFP-RPA1(L221P) resulted in S-phase and G_2-M populations similar to the RPA1-depleted phenotype (Fig. 2A, rightmost panel).

To determine whether the two expression plasmids were behaving similarly in HeLa cells, we compared the transfection efficiency of the two plasmids in four independent experiments. The average transfection efficiency of GFP-RPA1(L221P) plasmid was slightly lower than with the WT GFP-RPA1 plasmid; however, this difference was not statistically significant (Student's t test $P = 0.05$; Fig. 2B). The average green fluorescence per cell was also quantitated to determine the expression levels of the two forms of RPA1. There was significant variation in the protein level in individual cells (Fig. 2A, top row), but overall the average fluorescence of cells expressing GFP-RPA1 and GFP-RPA1(L221P) were not significantly different ($P = 0.18$; Fig. 2C). It has been shown previously that the level of expression of GFP-RPA1 obtained under these conditions is comparable with the endogenous levels of RPA1 (23). This shows that WT and L221P are expressed at similar levels in these experiments. We conclude that L221P did not complement the RPA1 depletion and that this mutant form is not able to support some essential function of the RPA complex.

Increased ChK2 phosphorylation in the presence of RPA1(L221P)

To determine whether the G_2-M accumulation observed in cells expressing L221P was due to initiation of a checkpoint, we assessed the activation of the checkpoint effector kinase, checkpoint protein 2 (ChK2; ref. 29). Cells expressing WT or L221P forms of RPA1 were stained with an antibody to phosphorylated ChK2 (p-Chk2) and analyzed by flow cytometry. Nontreated cells contained undetectable levels of p-Chk2 (Fig. 3A). Depletion of RPA1 resulted in two populations of cells: one with low p-ChK2 levels similar to nontreated cells and a second population with high levels of p-ChK2 (Fig. 3A). These two peaks probably correspond to cells that are in G_1 and cells that have an activated checkpoint after attempting to progress through S phase in the absence

Published OnlineFirst June 29, 2010; DOI: 10.1158/1541-7786.MCR-10-0161

of RPA1 triggering checkpoint activation, respectively. Expression of exogenous WT RPA1 restored low levels of p-ChK2, although the staining level of p-ChK2 in reconstituted cells was slightly elevated over nontreated cells (Fig. 3A). Reconstitution with RPA1(L221P) resulted in all cells having high levels of p-ChK2 (Fig. 3A). The elevated phosphorylation of ChK2 in cells expressing RPA1 (L221P) indicated activation of a cell cycle checkpoint

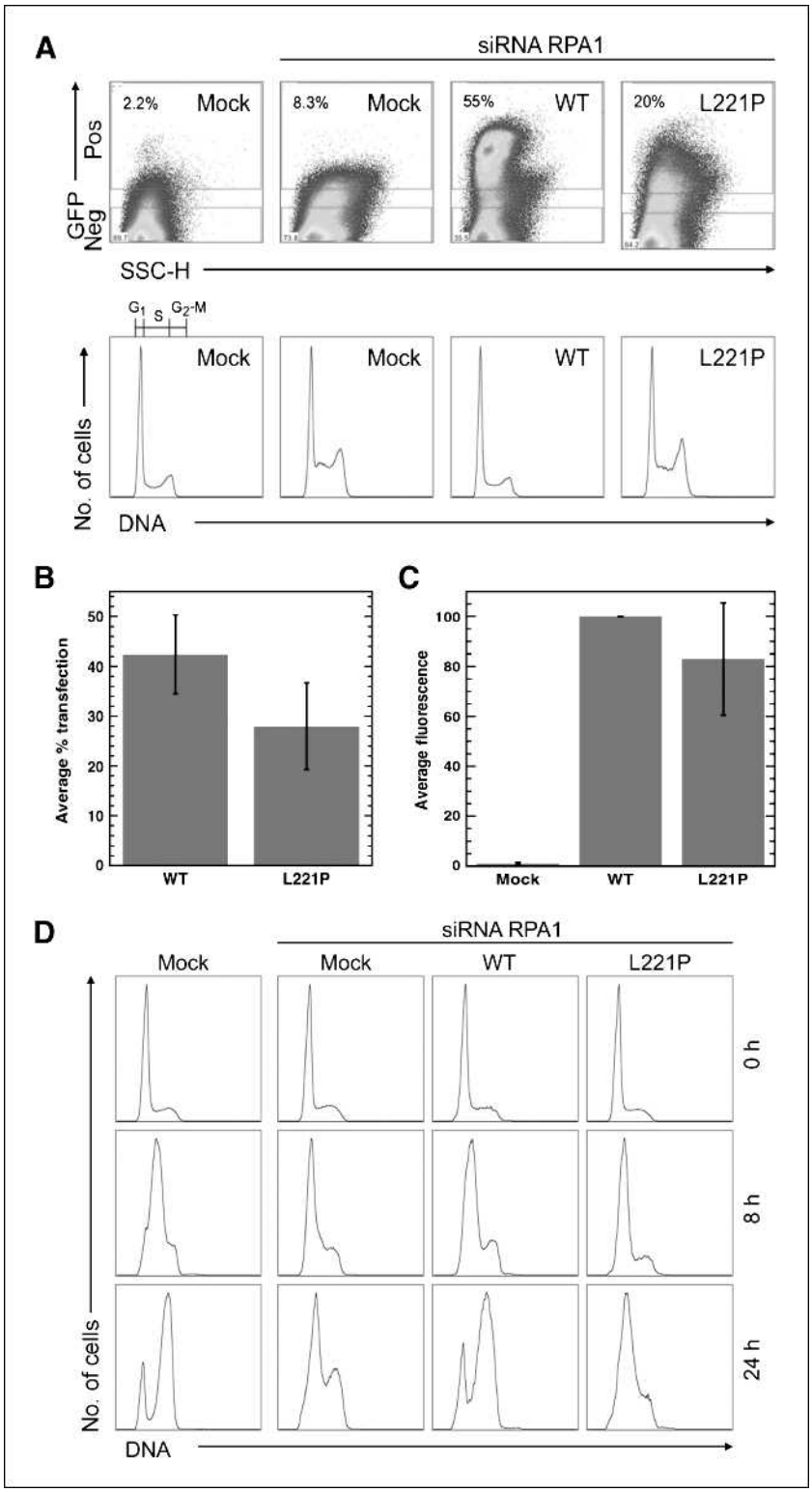

FIGURE 2. Effect of L221P on cell cycle progression. A, cells transfected with RPA1 siRNA and GFP-tagged WT or L221P RPA1 vector where indicated as described in Materials and Methods. At 96 h, DNA content was analyzed with flow cytometry. Top row, GFP expression (with % of GFP-positive cells indicated in top left corner); bottom row, DNA content as a histogram. B and C, analysis of the combined data from the experiment described in A and three similar, independent experiments. B, average transfection efficiency (GFP-positive cells) from cells treated with RPA1 siRNA and transfected with GFP-tagged WT or L221P RPA1 with SD between experiments shown (bars). C, average GFP fluorescence intensity average GFP fluorescence intensity for all GFP-positive cells (e.g., top box in A) was determined for mock-treated (mock) and for RPA1 siRNA-treated GFP WT or GFP-L221P and is shown with SD between experiments indicated (bars). Because gain settings varied between experiments, values from each experiment were normalized to WT RPA1 (WT). D, cells were treated and analyzed as described in A; at 96 h after mock or siRNA transfection, cells were synchronized with 5μg/mL aphidicolin for 24 h, then released into media. Flow cytometry was used to analyze DNA content at 0, 8, and 24 h after release. A and D, DNA content shown for GFP-negative cells for Mock samples and GFP-positive cells for WT and L221P.

Published OnlineFirst June 29, 2010; DOI: 10.1158/1541-7786.MCR-10-0161

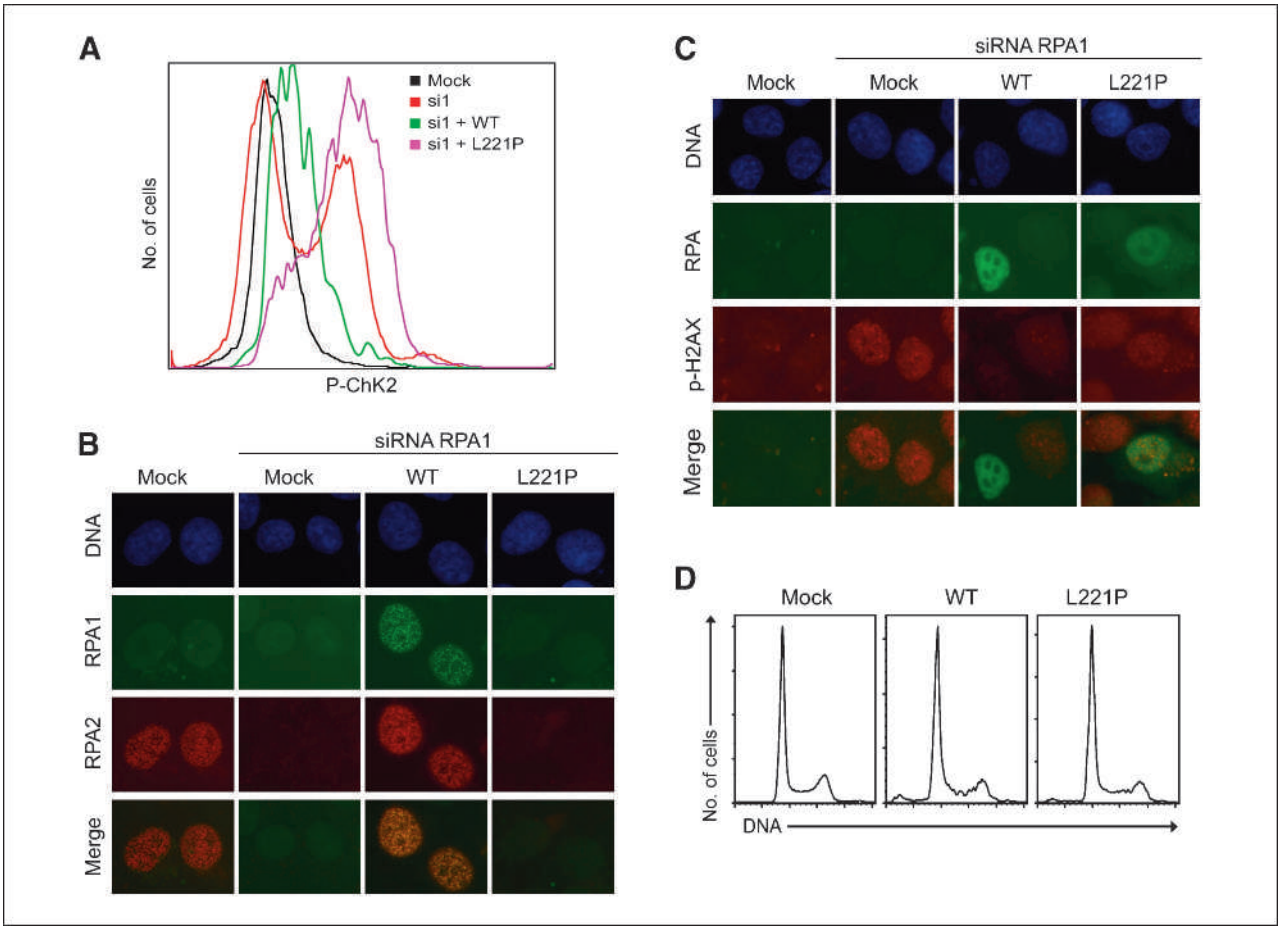

FIGURE 3. Cellular response to DNA damage. A, activation of ChK2 in the absence of induced DNA damage. At 96 h after mock or RPA1 siRNA transfection (si1), cells were stained for phosphorylated ChK2 and analyzed through flow cytometry. B, localization of WT and L221P mutant RPA complexes to sites of DNA damage. Cells were grown on coverslips and treated with 20 μmol/L camptothecin for 4 h. Nonchromatin-bound RPA was extracted before fixing slide. Row one, 4′,6-diamidino-2-phenylindole staining; row two, GFP-tagged RPA1; row three, RPA2 antibody staining; row four, merge of rows two and three. C, ability to recognize sites of DNA damage. Cells treated as in B. Row one, 4′,6-diamidino-2-phenylindole staining; row two, GFP-tagged RPA1; row three, stained with p-H2AX antibody; row four, merge of rows two and three. D, coexpression of L221P mutant and endogenous WT RPA1. Forty-eight hours after wells were seeded, the cells were mock transfected or transfected with GFP-tagged WT or L221P mutant RPA1 vector. At 96 h, DNA content of cells was stained with propidium iodide and analyzed through flow cytometry. GFP-negative cells were selected for mock samples; GFP-positive cells were selected for WT and L221P samples.

and was consistent with the altered cell cycle distribution observed in these cells (Fig. 2A).

RPA1(L221P) is unable to support progression through S phase

To directly examine cell cycle progression in cells expressing only RPA1(L221P), we analyzed a synchronized culture of RPA1(L221P)-expressing cells. Cells were synchronized with aphidicolin, an inhibitor of DNA polymerases, for 24 hours and released to allow resumption of cell cycle progression. The cell cycle distribution was assessed by propidium iodide staining and flow cytometry analysis at 0, 8, and 24 hours after release from aphidicolin treatment. At 0 hours the majority of the cellular population were in G_1 phase (Fig. 2D, top row). Mock-treated cells were able to resume progression into S phase indicated by the rightward progression of the peak at 8 hours (Fig. 2D, leftmost column). At 24 hours, most of the population had reached G_2-M phase and some had completed cell division and returned to G_1 phase (Fig. 2D, leftmost column). In cells lacking RPA1, only a small proportion of the population had begun to move into S phase indicated by the slight thickening of the G_1 peak at 8 hours, whereas the majority of cells remain in the G_1 peak even at 24 hours after release (Fig. 2D, second column). Cells reconstituted with exogenous WT RPA1 were able to progress into S phase as indicated by the rightward progression of the peak at the 8- and 24-hour time points (Fig. 2D, third column). Cells expressing only RPA1(L221P) did not progress into S phase. The cell cycle distribution in the RPA1(L221P) cells was similar to the RPA1-depleted cells: minimal change in the G_1 peak at 8 hours and a slight thickening of the G_1 peak at 24 hours after release from aphidicolin (Fig. 2D, fourth column). These results indicate that cells expressing

Published OnlineFirst June 29, 2010; DOI: 10.1158/1541-7786.MCR-10-0161

only RPA1(L221P) do not progress through S phase. Together with the results in unsynchronized cells, these data indicate the L221P mutation in RPA1 causes a disruption in the ability of cells to progress normally through cell cycle and suggests a defect in the ability to support cellular replication.

RPA1(L221P) is unable to localize to damage-induced foci

After DNA damage, WT RPA localizes to sites of DNA damage resulting in a punctuated staining pattern within the nucleus. These spots, termed DNA repair foci, contain proteins involved in DNA damage recognition and repair and are sites of DNA repair (30). We used fluorescent microscopy to assess whether RPA1(L221P) could localize to DNA repair foci after DNA damage. HeLa cells were treated with the topoisomerase inhibitor camptothecin for 4 hours to induce DNA damage. The nonchromatin-bound RPA was extracted before fixing the cells. No GFP staining was observed in cells not transfected with GFP-tagged RPA1 (Fig. 3B, second row, left two images). An antibody to RPA2 showed that the endogenous RPA complex was localized to repair foci in the mock-treated cells (Fig. 3B, third row, left image). No RPA2 staining was observed for the cells treated with RPA1 siRNA confirming that the RPA complex is not able to localize to repair foci in the absence of RPA1 (Fig. 3B, third row, second column). Exogenous GFP-tagged WT RPA1 was able to form the punctuated staining pattern in the nucleus, indicating localization to damage-induced foci (Fig. 3B, second row, third column). RPA2 colocalized with the WT RPA1, confirming the localization of the entire RPA complex as expected (Fig. 3B, third row, third column). In contrast, neither GFP-RPA1(L221P) nor RPA2 foci were observed after DNA damage in cells reconstituted with RPA1(L221P) (Fig. 3B, second and third row, leftmost image). GFP-RPA1(L221P) was expressed in cells at similar levels to GFP-RPA1 based on GFP fluorescence in cells treated in parallel but not extracted before microscopy (data not shown). These results indicate that the L221P mutation disrupts the ability of the RPA complex to localize to DNA repair foci, suggestive of a defect in DNA repair.

RPA1(L221P) causes elevated phosphorylation of H2AX

The previous experiments argue that the L221P mutation causes a defect in the ability of the RPA complex to function properly in DNA replication and repair. A lack of effective DNA replication and repair should be expected to cause an accumulation of DNA damage in cells. To test this hypothesis, we assessed the level of cellular DNA damage by measuring phosphorylation of the histone variant H2AX, a marker associated with DNA damage (31). Cells were stained with an antibody to p-H2AX. The fluorescent microscopy was carried out as described above except that the extraction step was omitted to enable identification of cells expressing RPA1(L221P). No p-H2AX staining was detected in the mock-treated cells (Fig. 3C, third row, left image). A significant level of p-H2AX staining was evident in cells lacking RPA1, indicating elevated cellular DNA damage (Fig. 3C, third row, second column). Only background levels of p-H2AX were detected in cells reconstituted with WT RPA1 (compare GFP-expressing cells to nontransfected cells in Fig. 3B, third column). Cells reconstituted with RPA1(L221P) exhibited significant p-H2AX staining, indicating elevated cellular DNA damage (Fig. 3B, fourth column). We conclude that RPA1(L221P) is unable to function in DNA repair and results in increased accumulation of DNA damage.

RPA(L221P) is not dominant over WT RPA

To investigate if the L221P mutation has a dominant phenotype, we assessed the effect of RPA1(L221P) expression in the presence of endogenous RPA in HeLa cells. Cells were mock treated or transfected with WT RPA1 or mutant RPA1(L221P) without siRNA treatment. Mock-treated cells showed a normal cell cycle distribution as expected (Fig. 3D, left). Introduction of exogenous WT RPA1 did not cause a detectable change in the cell cycle distribution (Fig. 3D, middle). Introduction of RPA1(L221P) also did not cause a disruption in the cell cycle distribution (Fig. 3D, right). This indicates that RPA1(L221P) is not dominant over endogenous WT RPA in a short-term assay. These results suggest that the abnormal cellular progression phenotype observed in Fig. 2 was caused by the absence of functional RPA.

RPA1(L221P) forms a stable RPA complex

We next analyzed the biochemical properties of RPA1(L221P). RPA1(L221P) was expressed in combination with the RPA2 and RPA3 subunits in *Escherichia coli* and purified as previously published (26). The RPA1(L221P) complex had identical chromatography properties as and was purified with similar yields to WT RPA (data not shown). The purified RPA1(L221P) complex contained all three subunit of RPA, although the RPA1(L221P) polypeptide seemed to migrate slightly slower than the WT RPA1 in SDS-PAGE (Fig. 4A, compare lanes and 1 and 2). The purified RPA1(L221P)-containing complex, termed RPA(L221P), was biochemically characterized to gain insight into the mechanism of the replication and repair defects observed in the cells.

RPA1(L221P) is unable to support replication *in vitro*

SV40 virus replication depends on one viral protein, large T antigen (Tag), and multiple cellular proteins including RPA (32). Replication of SV40 can be reconstituted *in vitro* using Tag, RPA, and HeLa cell extract depleted of RPA by ammonium sulfate fractionation (26). By adding different forms of RPA and monitoring DNA synthesis, it is possible to directly test activity in-DNA replication. The reactions lacking RPA, or RPA and Tag, showed background levels of synthesis (Fig. 4B). WT RPA stimulated DNA synthesis, but addition of

Published OnlineFirst June 29, 2010; DOI: 10.1158/1541-7786.MCR-10-0161

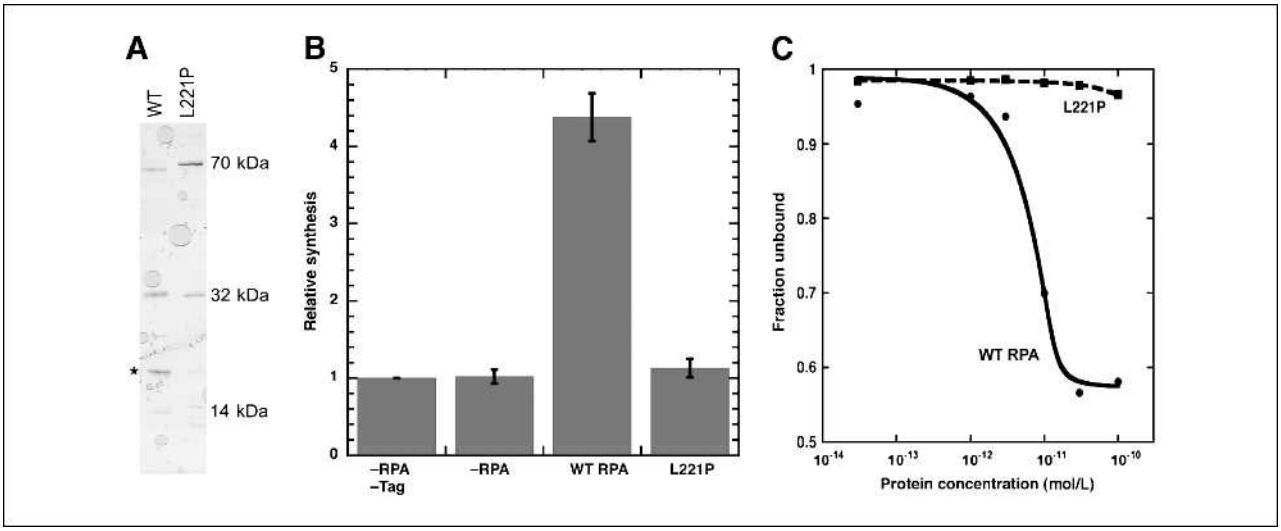

FIGURE 4. Biochemical properties of RPA-L221P. A, gel analysis of purified L221P RPA complex. One microgram of WT RPA or RPA containing the L221P RPA1 subunit were separated on an 8% to 14% SDS-PAGE gel and stained with silver nitrate. Lane 1, WT RPA; lane 2, L221P complex. *, non-RPA impurities. B, ability to support SV40 DNA replication *in vitro*. Background synthesis was assessed in the absence of RPA (–RPA) or Tag (–Tag). Synthesis of complete reactions containing 400 ng of either WT or L221P. A representative assay is shown; all reactions were done in duplicate and normalized to background. C, ssDNA binding. Binding isotherms of a representative gel mobility shift assay for WT and L221P complexes.

RPA(L221P) had no effect on the total DNA synthesis (Fig. 4B). These data confirm that RPA(L221P) is not able to support replication.

RPA1(L221P) is unable to bind ssDNA

To determine the molecular basis for the loss of activity in RPA(L221P), ssDNA binding activity was quantitated by gel mobility shift assay. WT RPA or RPA (L221P) were incubated with a radiolabeled ssDNA oligonucleotide, and the resulting complexes were separated using gel electrophoresis. The amount of free ssDNA and ssDNA-protein complex was quantitated. Figure 4C shows representative binding isotherms. WT RPA bound with high affinity and an apparent association constant of ~1×10^{12} mol/L^{-1}. In contrast, RPA(L221P) did not form a stable complex with ssDNA at any protein concentration tested (Fig. 4C). We estimated based on the highest concentration of RPA(L221P) used that these assays could have detected a binding affinity of $\geq 1 \times 10^{9}$ mol/L^{-1}. These results indicate that the L221P mutation reduces the ability of the RPA complex to bind ssDNA by at least 1,000-fold. The inability of RPA(L221P) to bind ssDNA explains the defect in DNA replication and repair. Together, the results show that the RPA1(L221P) is a nonfunctional form of RPA1, leading to a disruption in DNA replication and repair function of the RPA complex due to its inability to bind ssDNA.

Discussion

The L221P mutation seems to primarily affect the biochemical activity of RPA. The L221P mutation does not seem to affect the stability of recombinant RPA or the level of the RPA1 polypeptide expressed exogenously in the cells. However, L221P causes a dramatic decrease in the ssDNA binding activity of human RPA and results in a nonfunctional complex. Our studies show that L221 is important for normal DNA binding of RPA. These results provide a mechanism for why the homologous mutation in mice is homozygous lethal (25).

L221 is in DBD-A, one of two essential, high-affinity DBDs of RPA that are both necessary and sufficient for binding of the RPA complex to DNA (19, 20). The L221 residue is located in the center of the β-sheet that forms the ssDNA binding site (28). Modeling of a proline residue at position 221 predicted that it would cause a significant disruption of the β sheet (Fig. 1B). The DNA binding surface of DBD-A has been subjected to mutational analysis previously (19, 23). In these studies, it was shown that mutation of individual or pairs of DNA-interacting residues had only modest effects on ssDNA binding and resulted in functional forms of RPA (19, 23). In the only previously characterized form of DBD-A mutant that was nonfunctional, all six polar residues in DBD-A that interact with DNA were mutated to alanine (23). This form of RPA also had a dramatically reduced ssDNA binding activity (<0.1% of WT RPA). We conclude that the disruption of the core β sheet in DBD-A has a greater effect on DNA binding activity than do mutations that affect individual protein-DNA contacts.

Residue L221 is conserved in human, mice, and yeast. In addition, the structures and DNA interactions of the human and yeast DBD are very similar (Fig. 1A). However, in contrast to human cells and mice, yeast that are homozygous for L221P are viable (22, 24). Comparison of the β1-β2 strands in the two structures suggests a possible

Published OnlineFirst June 29, 2010; DOI: 10.1158/1541-7786.MCR-10-0161

explanation for this phenotypic difference. In human DBD-A, the β1 strand is discontinuous with three residues near L221 not part of the β sheet. In yeast, both β1 and β2 strands are continuous (Fig. 1B). This difference means that in the human protein, proline at position 221 is predicted to result in a long (approximately six residues) disruption of the β strand, whereas the same change in yeast results in a short (approximately three residues) disruption. We postulate that the shorter break in yeast allows the yeast protein to retain sufficient ssDNA binding activity to support life. Yeast containing L221P have an increase in sensitivity to DNA damage (22, 24) consistent with this mutation having only partial activity.

Genomic instability and a high cancer rate was observed in heterozygous mice with one allele of the homologous L221P mutation, but no loss of either the WT or the L221P allele was found when the tumors were analyzed. This was interpreted by Wang et al. (25) to indicate that the L221P mutant had a dominant phenotype. However, we see no evidence of a dominant phenotype when RPA1 (L221P) is expressed in RPA1-containing cells. We also find that the RPA complex containing RPA1(L221P) is nonfunctional *in vitro*. These results suggest that the genomic instability and high cancer rate observed in the heterozygous mice is caused by haploinsufficiency of RPA. It seems most likely that the expression of an inactive form of RPA from one allele causes a reduction in the cellular pool of functional RPA. In the long term, this leads to elevated levels of DNA damage, genome instability, and increased cancer development. Although many tumor suppressor genes require both alleles be nonfunctional to promote cancer (33), several genes including many of those directly involved in DNA repair cause an increase in the rate of cancer when only a single allele is inactivated (34). For example, haploinsufficiency of *BRCA1*, bloom syndrome helicase, or *RAD51* all lead to chromosome instability and/or elevated cancer rates (35-38). These studies provide evidence that haploinsufficency of RPA causes a similar phenotype.

Disclosure of Potential Conflicts of Interest

No potential conflicts of interest were disclosed.

Grant Support

American Heart Association Predoctoral Fellowship grant 09PRE2160147 (C.S. Hass), by a NIH Research Grant (GM44721).

The costs of publication of this article were defrayed in part by the payment of page charges. This article must therefore be hereby marked *advertisement* in accordance with 18 U.S.C. Section 1734 solely to indicate this fact.

Received 04/14/2010; revised 06/04/2010; accepted 06/07/2010; published OnlineFirst 06/29/2010.

References

1. Wold MS. Replication protein A: a heterotrimeric, single-stranded DNA-binding protein required for eukaryotic DNA metabolism. Annu Rev Biochem 1997;66:61–92.
2. Iftode C, Daniely Y, Borowiec JA. Replication protein a (RPA): the eukaryotic SSB. Crit Rev Biochem Mol Biol 1999;34:141–80.
3. Fanning E, Klimovich V, Nager AR. A dynamic model for replication protein A (RPA) function in DNA processing pathways. Nucleic Acids Res 2006;34:4126–37.
4. Kim HS, Brill SJ. Rfc4 interacts with Rpa1 and is required for both DNA replication and DNA damage checkpoints in *Saccharomyces cerevisiae*. Mol Cell Biol 2001;21:3725–37.
5. Dodson GE, Shi Y, Tibbetts RS. DNA replication defects, spontaneous DNA damage, and ATM-dependent checkpoint activation in replication protein A-deficient cells. J Biol Chem 2004;279:34010–4.
6. Zou Y, Liu Y, Wu X, Shell SM. Functions of human replication protein A (RPA): from DNA replication to DNA damage and stress responses. J Cell Physiol 2006;208:267–73.
7. Givalos N, Gakiopoulou H, Skliri M, et al. Replication protein A is an independent prognostic indicator with potential therapeutic implications in colon cancer. Mod Pathol 2007;20:159–66.
8. Tomkiel JE, Alansari H, Tang N, et al. Autoimmunity to the M(r) 32,000 subunit of replication protein A in breast cancer. Clin Cancer Res 2002;8:752–8.
9. Kumaran S, Kozlov AG, Lohman TM. *Saccharomyces cerevisiae* replication protein A binds to single-stranded DNA in multiple salt-dependent modes. Biochemistry 2006;45:11958–73.
10. Kim C, Snyder RO, Wold MS. Binding properties of replication protein A from human and yeast cells. Mol Cell Biol 1992;12:3050–9.
11. Kim C, Paulus BF, Wold MS. Interactions of human replication protein A with oligonucleotides. Biochemistry 1994;33:14197–206.
12. Sancar A, Lindsey-Boltz LA, Unsal-Kacmaz K, Linn S. Molecular mechanisms of mammalian DNA repair and the DNA damage checkpoints. Annu Rev Biochem 2004;73:39–85.
13. San Filippo J, Sung P, Klein H. Mechanism of eukaryotic homologous recombination. Annu Rev Biochem 2008;77:229–57.
14. Brill SJ, Stillman B. Replication factor-A from *Saccharomyces cerevisiae* is encoded by three essential genes coordinately expressed at S phase. Genes Dev 1991;5:1589–600.
15. Umezu K, Sugawara N, Chen C, Haber JE, Kolodner RD. Genetic analysis of yeast RPA1 reveals its multiple functions in DNA metabolism. Genetics 1998;148:989–1005.
16. Xu X, Vaithiyalingam S, Glick GG, Mordes DA, Chazin WJ, Cortez D. The basic cleft of RPA70N binds multiple checkpoint proteins including RAD9 to regulate ATR signaling. Mol Cell Biol 2008;28:7345–53.
17. Lao Y, Gomes XV, Ren YJ, Taylor JS, Wold MS. Replication protein A interactions with DNA. III. Molecular basis of recognition of damaged DNA. Biochemistry 2000;39:850–9.
18. Deng X, Habel JE, Kabaleeswaran V, Snell EH, Wold MS, Borgstahl GE. Structure of the full-length human RPA14/32 complex gives insights into the mechanism of DNA binding and complex formation. J Mol Biol 2007;374:865–76.
19. Wyka IM, Dhar K, Binz SK, Wold MS. Replication protein A interactions with DNA: differential binding of the core domains and analysis of the DNA interaction surface. Biochemistry 2003;42:12909–18.
20. Arunkumar AI, Stauffer ME, Bochkareva E, Bochkarev A, Chazin WJ. Independent and coordinated functions of replication protein A tandem high affinity single-stranded DNA binding domains. J Biol Chem 2003;278:41077–82.
21. Bochkarev A, Bochkareva E. From RPA to BRCA2: lessons from single-stranded DNA binding by the OB-fold. Curr Opin Struct Biol 2004;14:36–42.
22. Chen C, Umezu K, Kolodner RD. Chromosomal rearrangements occur in S. cerevisiae rfa1 mutator mutants due to mutagenic lesions processed by double-strand-break repair. Mol Cell 1998;2:9–22.
23. Haring SJ, Mason AC, Binz SK, Wold MS. Cellular functions of

Published OnlineFirst June 29, 2010; DOI: 10.1158/1541-7786.MCR-10-0161

human RPA1. Multiple roles of domains in replication, repair, and checkpoints. J Biol Chem 2008;283:19095–111.
24. Chen C, Kolodner RD. Gross chromosomal rearrangements in *Saccharomyces cerevisiae* replication and recombination defective mutants. Nat Genet 1999;23:81–5.
25. Wang Y, Putnam CD, Kane MF, et al. Mutation in Rpa1 results in defective DNA double-strand break repair, chromosomal instability and cancer in mice. Nat Genet 2005;37:750–5.
26. Binz SK, Dickson AM, Haring SJ, Wold MS. Functional assays for replication protein A (RPA). Methods Enzymol 2006;409:11–38.
27. Mason AC, Haring SJ, Pryor JM, Staloch CA, Gan TF, Wold MS. An alternative form of replication protein A prevents viral replication *in vitro*. J Biol Chem 2009;284:5324–31.
28. Bochkarev A, Pfuetzner RA, Edwards AM, Frappier L. Structure of the single-stranded-DNA-binding domain of replication protein A bound to DNA. Nature 1997;385:176–81.
29. Chaturvedi P, Eng WK, Zhu Y, et al. Mammalian Chk2 is a downstream effector of the ATM-dependent DNA damage checkpoint pathway. Oncogene 1999;18:4047–54.
30. Golub EI, Gupta RC, Haaf T, Wold MS, Radding CM. Interaction of human Rad51 recombination protein with single-stranded DNA binding protein, RPA. Nucleic Acids Res 1998;26:5388–93.
31. Dickey JS, Redon CE, Nakamura AJ, Baird BJ, Sedelnikova OA, Bonner WM. H2AX: functional roles and potential applications. Chromosoma 2009;118:683–92.
32. Hassell JA, Brinton BT. SV40 and polyomavirus DNA replication. In: DePamphilis ML, editor. DNA Replication in Eukaryotic Cells. Cold Spring Harbor: Cold Spring Harbor Laboratory Press; 1996 p. 639–77.
33. Sherr CJ. Principles of tumor suppression. Cell 2004;116:235–46.
34. Kerzendorfer C, O'Driscoll M. Human DNA damage response and repair deficiency syndromes: linking genomic instability and cell cycle checkpoint proficiency. DNA Repair (Amst) 2009;8:1139–52.
35. Tutt A, Ashworth A. The relationship between the roles of BRCA genes in DNA repair and cancer predisposition. Trends Mol Med 2002;8:571–6.
36. Rennstam K, Ringberg A, Cunliffe HE, Olsson H, Landberg G, Hedenfalk I. Genomic alterations in histopathologically normal breast tissue from BRCA1 mutation carriers may be caused by BRCA1 haploinsufficiency. Genes Chromosomes Cancer 2010;49:78–90.
37. Gruber SB, Ellis NA, Scott KK, et al. BLM heterozygosity and the risk of colorectal cancer. Science 2002;297:2013.
38. Date O, Katsura M, Ishida M, et al. Haploinsufficiency of RAD51B causes centrosome fragmentation and aneuploidy in human cells. Cancer Res 2006;66:6018–24.
39. Park CJ, Lee JH, Choi BS. Solution structure of the DNA-binding domain of RPA from *Saccharomyces cerevisiae* and its interaction with single-stranded DNA and SV40 T antigen. Nucleic Acids Res 2005;33:4172–81.
40. Eswar N, Eramian D, Webb B, Shen MY, Sali A. Protein structure modeling with MODELLER. Methods Mol Biol 2008;426:145–59.
41. Kabsch W, Sander C. Dictionary of protein secondary structure: pattern recognition of hydrogen-bonded and geometrical features. Biopolymers 1983;22:2577–637.

AACR American Association for Cancer Research

Molecular Cancer Research

Functional Characterization of a Cancer Causing Mutation in Human Replication Protein A

Cathy S. Hass, Lokesh Gakhar and Marc S. Wold

Mol Cancer Res 2010;8:1017-1026. Published OnlineFirst June 29, 2010.